PLOS | ONE

RESEARCH ARTICLE

Kv4.3-Encoded Fast Transient Outward Current Is Presented in Kv4.2 Knockout Mouse Cardiomyocytes

Jie Liu[1,2☯], Kyoung-Han Kim[1,2,3☯], Michael J. Morales[4], Scott P. Heximer[1], Chi-chung Hui[3,5*], Peter H. Backx[1,2*]

1 The Departments of Physiology and Medicine, University of Toronto, Toronto, Ontario, Canada, **2** Division of Cardiology, University Health Network, Toronto, Ontario, Canada, **3** Program in Developmental and Stem Cell Biology, Hospital for Sick Children, Toronto, Ontario, Canada, **4** Department of Physiology & Biophysics, University at Buffalo, the State University of New York, Buffalo, New York, United States of America, **5** The Departments of Molecular Genetics, University of Toronto, Toronto, Ontario, Canada

☯ These authors contributed equally to this work.
* cchui@sickkids.ca (CCH); p.backx@utoronto.ca (PHB)

OPEN ACCESS

Citation: Liu J, Kim K-H, Morales MJ, Heximer SP, Hui C-c, Backx PH (2015) Kv4.3-Encoded Fast Transient Outward Current Is Presented in Kv4.2 Knockout Mouse Cardiomyocytes. PLoS ONE 10(7): e0133274. doi:10.1371/journal.pone.0133274

Editor: Marcello Rota, Brigham & Women's Hospital—Harvard Medical School, UNITED STATES

Received: February 10, 2015

Accepted: June 25, 2015

Published: July 21, 2015

Data Availability Statement: All relevant data are within the paper and its Supporting Information files.

Funding: PHB received a grant (MOP 119339) from the Canadian Institutes for Health Research.

Competing Interests: The authors have declared that no competing interests exist.

Abstract

Gradients of the fast transient outward K^+ current ($I_{to,f}$) contribute to heterogeneity of ventricular repolarization in a number of species. Cardiac $I_{to,f}$ levels and gradients change notably with heart disease. Human cardiac $I_{to,f}$ appears to be encoded by the Kv4.3 pore-forming α-subunit plus the auxiliary KChIP2 β-subunit while mouse cardiac $I_{to,f}$ requires Kv4.2 and Kv4.3 α-subunits plus KChIP2. Regional differences in cardiac $I_{to,f}$ are associated with expression differences in Kv4.2 and KChIP2. Although $I_{to,f}$ was reported to be absent in mouse ventricular cardiomyocytes lacking the Kv4.2 gene (Kv4.2-/-) when short depolarizing voltage pulses were used to activate voltage-gated K^+ currents, in the present study, we showed that the use of long depolarization steps revealed a heteropodatoxin-sensitive $I_{to,f}$ (at ~40% of the wild-type levels). Immunohistological studies further demonstrated membrane expression of Kv4.3 in Kv4.2-/- cardiomyocytes. Transmural $I_{to,f}$ gradients across the left ventricular wall were reduced by ~3.5-fold in Kv4.2-/- heart, compared to wild-type. The $I_{to,f}$ gradient in Kv4.2-/- hearts was associated with gradients in KChIP2 mRNA expression while in wild-type there was also a gradient in Kv4.2 expression. In conclusion, we found that Kv4.3-based $I_{to,f}$ exists in the absence of Kv4.2, although with a reduced transmural gradient. Kv4.2-/- mice may be a useful animal model for studying Kv4.3-based $I_{to,f}$ as observed in humans.

Introduction

The fast transient outward potassium current ($I_{to,f}$) modulates action potential profile, Ca^{2+} handling, contractility and hypertrophy in cardiomyocytes [1, 2]. $I_{to,f}$ is also developmentally regulated [3] and its levels are invariably reduced in heart disease. Regional differences in $I_{to,f}$ are major determinants of the transmural gradient of ventricular repolarization in many

species [4, 5] and these gradients are often altered in diseased hearts [6]. The pore-forming α-subunits of $I_{to,f}$ channels are comprised of Kv4.2 and Kv4.3 in rodents [7], but apparently only Kv4.3 in humans [8]. In both case, they form oligomeric complexes with the obligatory auxiliary subunit KChIP2, as well as either DPP6 or DPP10 [7]. While the $I_{to,f}$ gradient in humans and dogs are linked to regional differences in KChIP2 expression [4, 9], the basis for regional differences in mouse $I_{to,f}$ is not clear with studies concluding that either Kv4.2 or KChIP2 or both underlie the transmural gradient [10].

In rodents, the molecular basis of $I_{to,f}$ is less clear. As $I_{to,f}$ was undetected in mice lacking the Kv4.2 gene, a previous report concluded that the native cardiac $I_{to,f}$ requires obligatory hetero-tetramers of Kv4.2 and Kv4.3 [11], even though $I_{to,f}$ currents are present in mice lacking Kv4.3 [12] and can be generated in heterologous expression systems by either Kv4.2 or Kv4.3 α-subunits alone [5]. While several molecular explanations could account for these conflicting findings, the previous studies [11, 12] used short depolarization pulses (lasting ~5 sec) to quantify $I_{to,f}$, which do not allow accurate dissection and quantification of K^+ currents in mouse cardiomyocytes [13, 14]. Recently, we showed that long depolarization pulses (lasting ~25 sec) are required to accurately dissect and quantify the different K^+ currents in mouse cardiomyocytes [12]. Therefore, we re-examined the existence of $I_{to,f}$ in mice lacking the Kv4.2 gene (Kv4.2-/-) and found clear evidence for the presence of $I_{to,f}$ in Kv4.2-/- hearts with a markedly reduced transmural gradient.

Materials and Methods

Transgenic animals and genotyping

All animal experiments were performed in accordance with protocols approved by the Faculty of Medicine and Pharmacy Animal Care Committee, University of Toronto, and conformed to the standards of the Canadian Council on Animal Care. Mice lacking of Kv4.2 gene (K_V4.2-/-) [11] were bred into a C57/B6 background. Heterozygous-heterozygous breeding was used to generate Kv4.2-/- and wild-type (WT) littermates. Genotyping was performed using the following primers: K_V4.2 (613 bps; forward, GTGGAT GCC TGT TGC TTC; reverse, CCC ACA AGG CAG TTC TTT TA) and aminoglycoside phosphotransferase (neomycin-resistance) (500 bps; forward, AGG ATC TCC TGT CAT CTC ACC TTGCTC CTG; reverse, AAG AAC TCG TCA AGA AGG CGA TAG AAG GCG) [15].

Isolation of Adult Mouse Ventricular Myocytes

As previously described [13], hearts were rapidly removed from anesthetized (4% isoflurane oxygen mixture inhalation) mice and retrogradely perfused with Ca^{2+}-free Tyrode's solution, which contained (in mM): 137 NaCl, 5.4 KCl, 1.0 $MgCl_2$, 0.33 NaH_2PO_4, 10 D-glucose, 10 HEPES, pH 7.4, at 37°C through aorta for 3–4 min. Then it was perfused with collagenase (Type II, 1.0 mg/mL, Worthington) for 10–12 min. The EPI and ENDO heart cells were collected with a sharp forceps under a dissecting microscope. After heart was digested, the right ventricle was removed and an incision was made into the ventricular septum in order to expose the endocardium (ENDO) of the left ventricular free wall. A small amount of ENDO tissue (~0.05mm^3) was collected from left ventricular free wall inner surface at the level of the tip of papillary muscle. Then the outside surface of left ventricular was washed with Krebs bicarbonate solution and a small amount (~0.05mm^3) of EPI tissue was picked up from the middle point of left ventricular free wall. The digested ventricular tissue was gently triturated in the cell storage solution, which contained (in mM): 120 potassium glutamate, 20 KCl, 20 HEPES, 1.0 $MgCl_2$, 10 D-glucose, 0.5 K-EGTA, and 0.1% bovine serum albumin.

Patch Clamp Electrophysiology & Data Analysis

Voltage-activated K^+ currents from isolated ventricular myocytes were recorded with the whole-cell patch clamp technique (Axopatch 200B and Clampex8 software, Axon Instrument, CA, USA) at room temperature (24°C). Measurements were made at room temperature in order to facilitate comparisons with previous studies in which voltage-gated K^+ currents were quantified in mouse cardiomyocytes [4, 7, 11, 16, 17] and in particular to allow comparisons with our previous study wherein a method was developed to reliably dissect voltage-gated K^+ currents in mouse cardiomyocytes [13]. Cells were perfused with bath solution for 15 minutes before electrophysiological recording. Ca^{2+} tolerant rod-shape cardiomyocytes were selected and examined. The bath solution contained (in mM): 140 NaCl, 4 KCl, 1 $MgCl_2$, 1.2 $CaCl_2$, 10 HEPES, 10 D-glucose, and 0.3 $CdCl_2$ (pH 7.4). The pipette resistance ranged between 1.2~2.0 MΩ when filled with a pipette solution, which contained (in mM): 120 potassium aspartate, 20 KCl, 10 NaCl, 1 $MgCl_2$, 5 MgATP, 10 HEPES, and 10 EGTA (pH 7.2). Cell capacitance and series resistance were electronically compensated by 85%. Voltage-gated K^+ currents were induced with a 25 second depolarization from a holding potential of -80 mV to +60 mV, at which membrane potential K^+ channels are fully activated and also minimize the contributions of potential overlapping Na^+ currents. A double-pulse protocol was used for characterizing K^+ currents recovery from inactivation kinetics. Cells were first depolarized to +60 mV for 20 sec (pre-pulse), subsequently hyperpolarized to the holding potential at -80 mV for various times ranging from 10 ms to 6 sec, and then stepped to +60 mV for another 5–20 sec (test-pulse) to activate the currents and assess the extent of recovery; sweep interval was set at 45 sec for full recovery of all K^+ currents and allow sufficient time to adequately check and adjust (as required) the series-resistance compensation and resting membrane potential before each subsequent depolarization. HpTx-2 (5 μM) was used in bath solution for certain experiments.

Electrophysiological data were analyzed using pClamp software (Clampfit9, Axon, CA, USA). Inactivation of voltage-dependent outward K^+ currents was fitted with a sum of three exponentials:

$$f(t) = A_1 e^{-t/\tau_1} + A_2 e^{-t/\tau_2} + A_3 e^{-t/\tau_3} + \mathrm{C} \quad (1)$$

Here, A is the current amplitude, τ is inactivation time constant, C is non-inactivate current component (I_{ss}). The goodness of fitting was evaluated by the correlation coefficients (R value).

To quantify the recovery of I_{to} in mouse cardiomyocyte, I_{to} in both pre-pulse and test-pulse were dissected from I_{Kslow1}, I_{Kslow2} and I_{ss} with 3-exponential curve fitting. I_{to} in test-pulse was normalized to that in pre-pulse, and the ratio was plotted as a function of pulse interval time and fit with a biphasic equation:

$$I/I_0 = A_1(1 - e^{-\frac{t}{\tau_1}}) + A_2(1 - e^{-\frac{t}{\tau_2}}) \quad (2)$$

Here A is percentage of each component in whole current ($A_1 + A_2 = 1$), τ is the recovery time constant.

Immunofluorescent staining

Immunofluorescent staining was performed as previously described [18]. In brief, isolated myocytes were plated on laminin-coated (0.5 mg/mL, Roche) glass coverslips, fixed with 4% paraformaldehyde in PBS for 1 hour at room temperature, and permeated with 0.2% (v/v) Triton X-100 for 10 min. After blocking with 1% bovine serum albumin in PBS, cells were exposed to primary antibody against Kv4.3 (1:100) in blocking solution overnight at 4°C. The anti-Kv4.3 mouse monoclonal antibodies (NeuroMab) were raised against a fusion protein

corresponding to amino acids 415–636 in the cytoplasmic C-terminus of a rat Kv4.3 protein [19]. A secondary Alexa Fluor 488 goat anti-mouse IgG (Invitrogen) was subsequently used for visualization. Images were acquired with an argon laser beam equipped confocal microscope (excitation 488nm, emission 519nm; Olympus). To control for background and cell auto-fluorescence, parameters were normalized based on fluorescence intensities measured in control samples containing no antibody, primary antibody only or secondary antibody. The Kv4.3 expression was quantified by the average fluorescence signals in 3-dimensional reconstructions of immunofluorescence images of isolated myocytes obtained using optical Z sections (0.5 μm thickness) with a 60X magnification oil objective in conjunction with a Kalman filter (n = 3). The distribution of fluorescence density across the cells in the middle layer image was analyzed. 3D construction was performed using ImagePro Plus (Media Cybernetcis).

Quantitative RT-PCR

Total RNA was isolated with TRIZOL reagent (Life Technologies), and then cDNA was synthesized from 1.0 μg of RNA using Superscript II reverse transcriptase (Life Technologies). The samples from different regions of the heart (i.e. left ventricular epicardium and endocardium) were obtained by dissection from the left ventricular free wall using a scalpel with the aid of a dissecting microscope. Gene expression assay was conducted on 10 ng of template cDNA by Quantitative PCR (qPCR) using Taqman and SYBR green PCR methods equipped with ABI 7900HT (Applied Biosystems). Primers for mouse *Kcnd2* (Kv4.2), *Kcnd3* (Kv4.3) and *Kcnip2* (KChIP2) are as follows: *Kcnd2* forward, 5'-GTGTCGGGAAGCCATAGAGGC-3', Reverse, 5'-TTACAAGGCAGACACCCTGA-3'; *Kcnd3* forward, 5'-CTCCCGTCGTAGCAAGAAGA-3', Reverse, 5'-GGTGGGGATGCTGATGATG-3'; and *Kcnip2* forward, 5'-GGCTGTATCAC GAAGGAGGAA-3', Reverse, 5'- CCGTCCTTGTTTCTGTCCATC-3'. The relative expression of these genes was determined using the normalized comparative CT method [20] with *Gapdh* as the background gene, which did not vary between regions. The total cycle numbers for all experiments was 35 and the products were verified using both melt tests and agarose gels. Thresholds were determined from the linear regions of the amplification curves and the efficiency of the probes was estimated using serial dilutions.

Statistics

All results were expressed as Mean ± S.E.M. Statistical significance of differences were determined by Student's *t* test (paired or unpaired) and ANOVA. Differences at $P< 0.05$ were considered statistically significant. Calculations and statistical tests were performed using Prism5.03 (GraphPad Software, San Diego, CA, USA).

Results

$I_{to,\ f}$ is present in Kv4.2-/- endocardial myocytes (ENDO)

Voltage-dependent K+ currents in mouse cardiomyocytes are generated by Kv4.2/Kv4.3, Kv1.4, Kv1.5 and Kv2.1-encoded channels [4, 14, 16, 17, 21–27]. Currents generated by Kv4.2/Kv4.3 and Kv1.4 channels have similar activation and inactivation kinetics (fast), with inactivation time constants (τ_{inact}) < 150 ms; while the τ_{inact} of Kv1.5 and Kv2.1 channels are ~800 ms (intermediate) and ~4500 ms (slow), respectively. Based on these biophysics features, previous studies have established that voltage-gated K^+ currents, when stimulated from rest with depolarizing pulses lasting 25 sec, are best described with 3-exponential function and four temporal components are dissected: a sustained component (i.e. I_{sus}), a "slow" component (i.e. $I_{K,slow2}$ probably encoded by Kv2.1), an "intermediate" component (i.e. $I_{K,slow1}$ probably encoded by

Kv1.5), and a "fast" component (i.e. I_{to}) which can be further separated, using recovery from inactivation protocols based on their significantly different recovery kinetics, into an $I_{to,f}$ (encoded by Kv4.2/3) and an $I_{to,s}$ (encoded by Kv1.4-encoded) component [13]. Fig 1A shows K^+ currents recorded using 25 sec depolarizing pulses (to +60mV) from a holding potential of -80mV recorded in wild-type (WT) and Kv4.2-/- cardiomyocytes. As reported previously, the outward K^+ currents in WT cardiomyocytes (isolated from the ENDO) are well fit with tri-exponential functions (R-value range was 0.976–0.995, 88% of R-values were > 0.98). Cardiomyocytes from Kv4.2-/- mouse hearts could be similarly fit well with tri-exponential functions and we found no differences in either the amplitudes or decay (i.e. inactivation) kinetics of the $I_{k,slow1}$, $I_{k,slow2}$ and I_{sus} components between the groups (Fig 1B and Table 1). On the other hand, the current density of the fastest decaying component (i.e. I_{to}) was reduced ($P<0.0001$) in Kv4.2-/- ENDO myocytes (6.89 ± 0.44 pA/pF, n = 21) compared to WT (11.80 ± 0.82 pA/pF, n = 20) (Fig 1C and Table 1). Recovery from inactivation of the fastest decaying component (i.e. I_{to}) yields a bi-exponential time course (Fig 2 and Table 2) with the fast recovering portion (i.e. $I_{to,f}$) having a lower ($P<0.0001$) density in Kv4.2-/- ENDO cardiomyocytes (3.21 ± 0.31 pA/pF, n = 12) compared to WT (7.69 ± 0.87 pA/pF, n = 12) without differences ($P = 0.9111$)

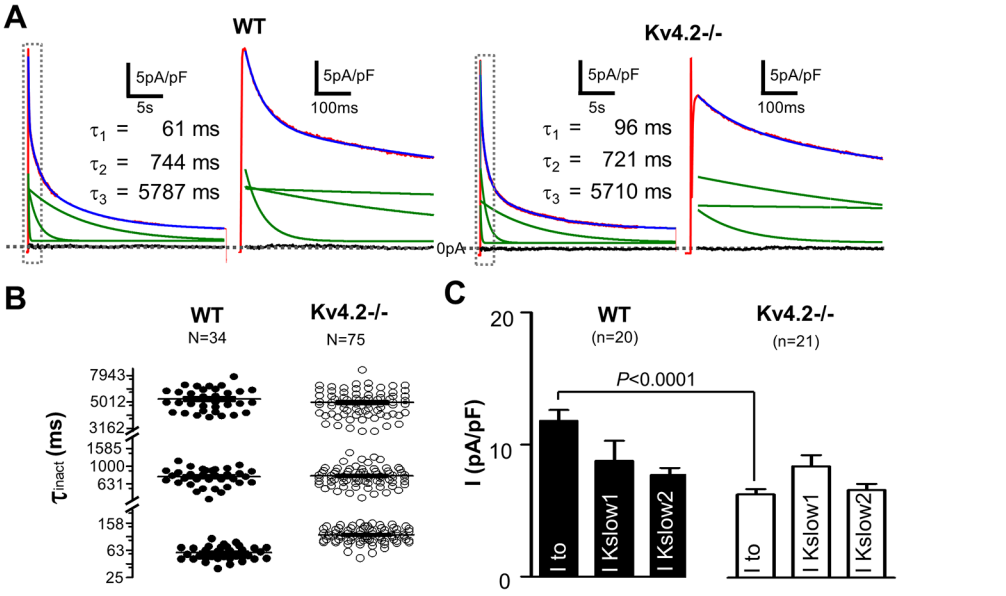

Fig 1. Outward K^+ currents measured in ENDO cardiomyocytes isolated from WT and Kv4.2 -/- hearts. (A) Typical outward K^+ currents measured in both the WT and Kv4.2-/- are shown following step depolarization to +60mV (for 25s) from a holding potential of -80mV. The 2nd and 4th panels are 50-folds time expanded relative to the area in the boxes on their left side adjacent panels (1st and 3rd panels). Voltage-dependent K^+ currents recorded from both groups of cardiomyocytes could be well fit with tri-exponential functions (show in blue). The three green lines in each panel represent the three individual components of the tri-exponential functions, and their time constant (t) are shown in the inset tables. The residuals (i.e. the differences between the red and blue curves) are also shown in black and, as can be seen, these residuals are essentially zero consistent with the very high correlation coefficients (R-values) typically estimated in the fits of all our traces (which ranged from 0.976–0.995 with 88% of R-values being > 0.98). (B) Summary of the predicted inactivation time constants of the three individual exponential components of the tri-exponential functions that provided the best fit for all K^+ current traces analyzed. These three components were labeled based on their kinetics as: I_{Kslow2} (slowest), I_{Kslow1} (intermediate) and I_{to} (fastest). We previously demonstrated that tri-exponential fits provide optimal fits to the outward K^+ currents thereby allowing the different underlying current to be quantified in detail[21]. Notice that the kinetics (i.e. the τ value) of I_{Kslow2} and I_{Kslow1} are unchanged while kinetics of I_{to} are slower ($P<0.0001$) in Kv4.2-/- than WT. This shift in the kinetics of I_{to} is explained and discussed further in the text. C) Shows the current densities for I_{Kslow2}, I_{Kslow1} and I_{to} in WT and Kv4.2-/- cardiomyocytes estimated from the amplitudes of the three kinetic K^+ current components (obtained from the fits to the individual current traces). As can be seen that I_{to} density was much smaller, as expected, in Kv4.2-/- compared to WT while $I_{K,slow2}$ and $I_{K,slow1}$ are comparable between WT and Kv4.2-/-.

doi:10.1371/journal.pone.0133274.g001

Table 1. Comparison of potassium current density and relative amplitude in ventricular myocyte.

		I_{to}	I_{Kslow1}	I_{Kslow2}	I_{sus}
ENDO					
WT	Density (pA/pF)	11.80±0.82	8.78±1.51	7.71±0.52	4.67±0.34
n = 20	Amplitude (%)	36±0.31	27±0.62	24±0.54	13±0.29
Kv4.2-/-	Density (pA/pF)	6.89±0.44*	9.23±0.91	7.25±0.51	4.02±0.55
n = 21	Amplitude (%)	24±0.27	33±0.42	26±0.37	17±0.41
EPI					
WT	Density (pA/pF)	28.37±1.21*	33.45±2.95*	18.52±1.77*	7.33±0.57*
n = 14	Amplitude (%)	32±0.86	38±0.40	21±0.96	9±0.37
Kv4.2-/-	Density (pA/pF)	8.96±0.78^#	31.12±1.88^#	10.98±0.63^#	4.39±0.28^
n = 54	Amplitude (%)	17±0.51	56±0.45	20±0.84	7±0.23

* P<0.05, compared to WT ENDO

^ P<0.05, compared to WT EPI

# P<0.05, compared to Kv4.2-/- ENDO

doi:10.1371/journal.pone.0133274.t001

in slower component (i.e. $I_{to,s}$). These findings support the conclusion that $I_{to,f}$ is present in Kv4.2-/- cardiomyocytes but at reduced levels compared to WT without changes in the other

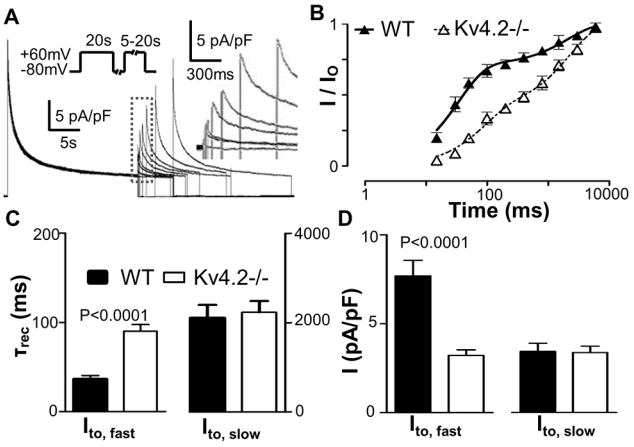

Fig 2. Recovery from inactivation kinetics of I_{to} (i.e. the fastest inactivation component of the outward K^+ currents) in WT and Kv4.2-/-cardiomyocyte. (A) Shows representative K^+ current recovery from inactivation recordings from a typical Kv4.2-/- cardiomyocyte. See Methods for the specific protocol. The early portions of traces following the depolarizing test-pulse are re-shown on a faster (expanded to 300 ms/bar scale) time scale in the inset (broken box) to better illustrate the properties of the time-course (of the recovery) of the peaks of the I_{to} K^+ currents as a result of membrane repolarization (to -80mV). (B) This panel shows the normalized I_{to} current as a function of the pulse interval duration during the recovery from inactivation protocol. The normalized current is defined as the amplitude of the I_{to} density (i.e. the fastest component) estimated from fits to the currents elicited following depolarization during the recovery period (as described in Fig 1) divided by the I_{to} density (i.e. fastest component) estimated from fits of the current measured following depolarization during the initial conditioning pulse. Notice that the time course of the recovery of the I_{to} current shows clear bi-phasic properties, as we described previously, in ENDO cardiomyocytes from WT and Kv4.2-/- hearts. This bi-phasic recovery property of I_{to} clearly indicates that I_{to} induced following depolarization is comprised of two underlying currents with different recovery kinetics, a fast recovery component ($I_{to,f}$) and a slow component ($I_{to,s}$). (C) This shows a summary of the kinetics of the biphasic recovery (i.e. τ_{rec}) allowing separation into $I_{to,f}$ and $I_{to,s}$. Note that the τ_{rec} for $I_{to,f}$ is increased and while that for $I_{to,s}$ is unchanged in Kv4.2-/- compared to WT. (D) Shows the estimated current density of $I_{to,\,f}$ and $I_{to,\,s}$ calculated from the relative proportions of the I_{to} recovering quickly or slowly from inactivation, respectively. Note that Kv4.2-/- decreases $I_{to,f}$ but not $I_{to,\,s}$.

doi:10.1371/journal.pone.0133274.g002

Table 2. Comparison of I_{to} recovery from inactivation in ventricular myocytes.

		$I_{to,f}$	$I_{to,s}$
ENDO without HpTx-2			
WT	τ_{rec} (ms)	33±3	2256±292
n = 12	Density (pA/pF)	7.69 ± 0.87	3.78±0.50
	Amplitude (%)	67±9	33±9
Kv4.2-/-	τ_{rec} (ms)	88±10^	2267±217
n = 12	Density (pA/pF)	3.21±0.31^ #	3.71±0.39
	Amplitude (%)	45±7	55±7
ENDO with HpTx-2 (5 μM)			
WT	τ_{rec} (ms)		1906±263
n = 6	Density (pA/pF)		4.36±0.93
Kv4.2-/-	τ_{rec} (ms)		2050±190
n = 6	Density (pA/pF)		4.13±0.75
EPI without HpTx-2			
WT	τ_{rec} (ms)	32±4 #	2187±277
n = 12	Density (pA/pF)	27.46±1.38^ #	0.63± 0.40^ #
	Amplitude (%)	98±1	2±1
Kv4.2-/-	τ_{rec} (ms)	86±4	2227±310
n = 12	Density (pA/pF)	4.64±0.28	3.92±0.41
	Amplitude (%)	56±7	44±7

^: P<0.05 compared to WT ENDO

#: P<0.05 compared to Kv4.2-/- EPI.

doi:10.1371/journal.pone.0133274.t002

voltage-gated K^+ currents in ENDO myocyte. It is worthy note that the estimated rate of decay (i.e. τ_{inact}) of the fastest component (i.e. $I_{to} = I_{to,f} + I_{to,s}$) was faster ($P<0.0001$) in WT cardiomyocytes (58 ± 2 ms, n = 34) than in Kv4.2-/- cardiomyocytes (106 ± 3 ms, n = 75) which parallels differences in inactivation kinetics between Kv4.2 versus Kv4.3 currents in heterologous expression systems [22, 28, 29], as discussed further below.

To confirm the presence of $I_{to,f}$ in Kv4.2-/- myocytes, we applied the specific blocker of Kv4.2/3 channels, HpTx-2. As showed in Fig 3, HpTx-2 (5 μM) only affected K^+ currents in first ~400 ms following the depolarization and reduced ($P = 0.0062$) the fast component of the voltage-gated K^+ currents (i.e. I_{to}) in ENDO cardiomyocytes by 3.0 3± 0.67 pA/pF (n = 6) in Kv4.2-/- cardiomyocytes (Fig 3), without affecting $I_{to,s}$, $I_{k,slow1}$, $I_{k,slow2}$ or I_{sus}.This extent of I_{to} reduction is remarkably similar to ($P = 0.7841$) to the $I_{to,f}$ density estimated from fits to the fastest kinetic component in recovery from inactivation voltage protocols (i.e. 3.21 ± 0.31 pA/pF), as summarized in Table 2. In addition, the decay kinetics (τ_{inact}) of HpTx-2-sensitive current displayed a mono-exponential time course in both groups with τ_{inact} being larger ($P<0.0001$) in Kv4.2-/- cardiomyocytes (85 ± 11 ms, n = 6) than in WT (53 ± 6 ms, n = 5). Consistent with these results, HpTx-2 blocked the fast recovery component (i.e. $I_{to,f}$) in both WT and Kv4.2-/- cardiomyocytes without affecting the slow component ($I_{to,s}$). Specifically, as summarized in Table 2, I_{to} recovery from inactivation in Kv4.2-/- followed a mono-exponential time course in the presence of 5 μM HpTx-2 with a time constant (τ_{rec} = 2050 ± 190 ms, n = 6, R = 0.9939) which was indistinguishable ($P = 0.8112$) to the estimated τ_{rec} for $I_{to,s}$ (2267 ± 217 ms, n = 12, R = 0.9950) when HpTx-2 was absent. Similarly, in WT cardiomyocytes, τ_{rec} was estimated to be 1906 ± 263 ms (n = 6, R = 0.9862) in the presence HpTx-2 which did not differ ($P = 0.7769$) from τ_{rec} for the slow recovering component (2256 ± 292 ms, n = 12, R = 0.9878)

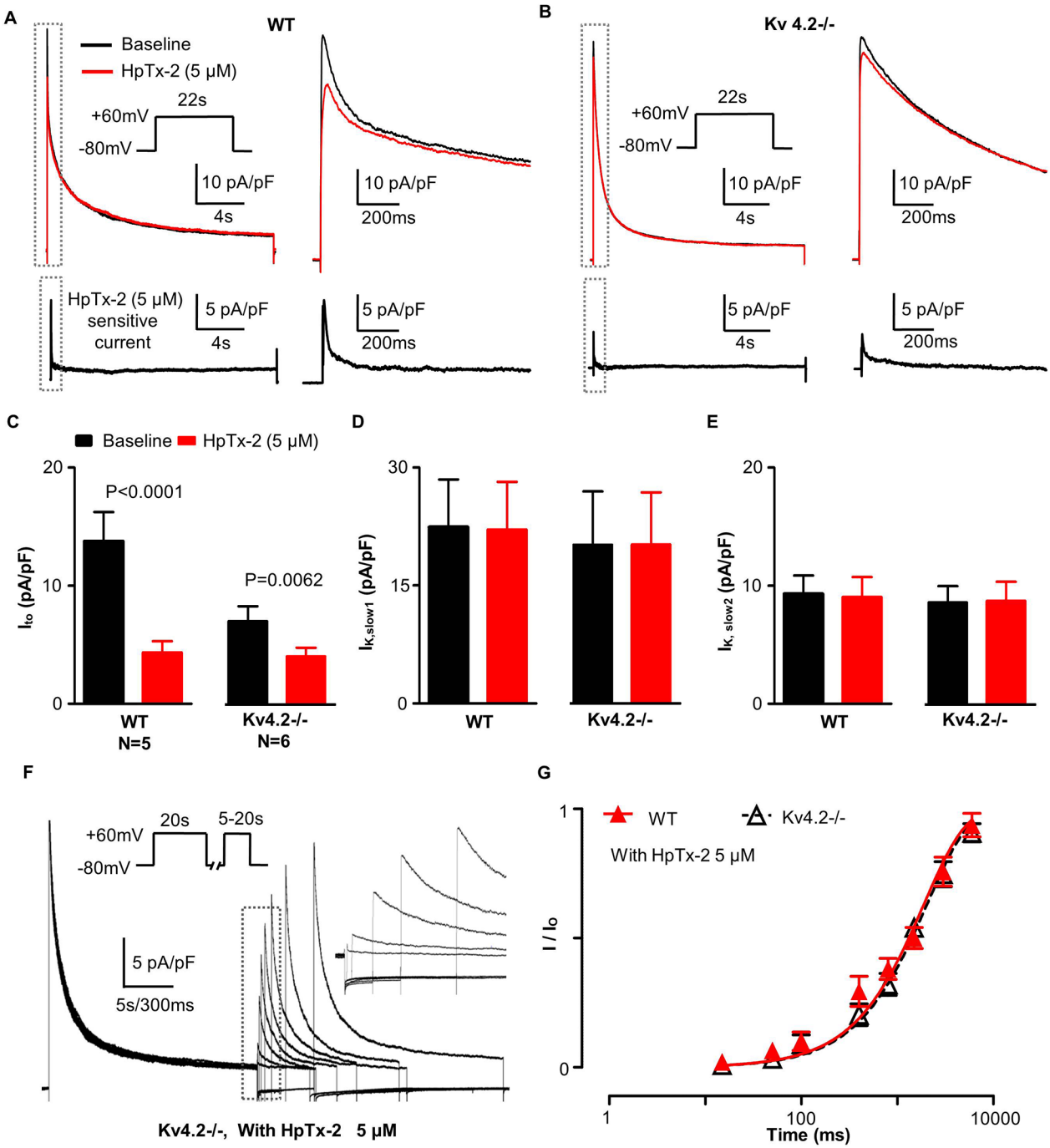

Fig 3. Effect of HpTx-2 on K+ current from isolated WT and Kv4.2-/- cardiomyocyte. (A) This panel illustrates representative K^+ current traces recorded from isolated WT cardiomyocyte under baseline (dark) conditions and after the addition of 5 μM HpTx-2 (red), a high-selective Kv4.x channel blocker. The HpTx-2 sensitive current was obtained by arithmetic subtraction of the red trace (with HpTx-2) from the dark trace (baseline) control and is shown in the lower trace. The initial parts of traces (gray dashed box) are shown on a more rapid time scale on their right side. (B) Shows representative K^+ current traces from a Kv4.2-/- cardiomyocyte under baseline (dark) conditions and after the addition of 5 μM HpTx-2 (red). The HpTx-2 sensitive currents are shown in the lower trace. (C) Show here is the I_{to} current density estimated under both baseline conditions and after HpTx-2 treatment from the tri-exponential curve fits to the K^+ currents recorded (as described in Fig 1). Note that while HpTx-2 decreased the I_{to} current in both WT and Kv4.2-/-, the decrease was far greater ($P<0.01$) in WT than the Kv4.2-/- cardiomyocytes. (D) and (E) These panels show $I_{K,\ slow1}$ and $I_{K,\ slow2}$ current density estimated (using the curve fitting methods) under baseline conditions and after HpTx-2 addition. After HpTx-2 these two currents density remained fixed and did not differ between WT and Kv4.2-/- cardiomyocytes. (F) Shows representative K^+ current recovery from inactivation recordings from a typical Kv4.2-/- cardiomyocyte with 5 μM HpTx-2. See Methods for the specific protocol. The early portions of traces following the depolarizing test-pulse are re-shown on a faster (expanded to 300 ms/bar scale) time scale in the inset (broken box) to better illustrate the properties of the time-course (of the recovery) of the peaks of the I_{to} K^+ currents as a result of

membrane repolarization (to -80mV). (G) This panel shows the normalized I_{to} current as a function of the pulse interval duration during the recovery from inactivation protocol with 5 μM HpTx-2. The normalized current is defined as the amplitude of the I_{to} density (i.e. the fastest component) estimated from fits to the currents elicited following depolarization during the recovery period (as described in Fig 1) divided by the I_{to} density (i.e. fastest component) estimated from fits of the current measured following depolarization during the initial conditioning pulse. Notice that, the recovery of I_{to} in both WT and Kv4.2-/- here are similar and are best fit with mono-exponential equation without the fast recovery component (that is, $I_{to,f}$) showed in Fig 2B. Moreover, they were comparable to the slow components (that is, $I_{to,s}$) dissected in Fig 2B without HpTx-2.

doi:10.1371/journal.pone.0133274.g003

without HpTx-2. Finally, no differences in τ_{rec} of the slow recovering components of I_{to} were observed between Kv4.2-/- and WT with ($P = 0.6214$) or without ($P = 0.8611$) HpTx-2 (Table 2).

Expression of Kv4.3 α-subunit at the plasma membrane of myocytes

Although as expected Kv4.2 protein was not detected in Kv4.2-/- myocardium[11], Kv4.3 protein is expressed in Kv4.2-/- myocardium even though $I_{to,f}$ was failed to be detected using the short depolarization pulses (lasting ~5 sec) method[11], and these observations were considered as key to conclusion that Kv4.2 is required for functional integration of Kv4.3-based channels into the cardiomyocyte membrane[11]. However, in heterologous expression systems Kv4.3 alone generates $I_{to,f}$ and is inserted into cell membrane[23, 30]. We therefore performed immunofluorescent staining with Kv4.3 antibodies. As can be seen, from longitudinal and transverse three-dimensional reconstructions of isolated cells labeled with Kv4.3 antibodies (with the appropriate secondary antibodies), Kv4.3 α-subunits are clearly present at the membrane as indicated by the higher fluorescent density at the periphery of the cell than cell interior in both WT and Kv4.2-/- ventricular myocytes (Fig 4). The average fluorescent density in the periphery were comparable ($P = 0.4886$) between WT (99.17 ± 5.32, n = 9) and Kv4.2-/- (95.20 ± 2.91, n = 13).

I_{to} heterogeneity in the ventricular free wall of Kv4.2-/-

The results above support the conclusion that Kv4.3 α-subunits can form homotetrameric functional channels and generate $I_{to,f}$ in mouse cardiomyocytes when Kv4.2 is absent. Since the transmural $I_{to,f}$ gradients in mouse myocardium have been linked to variations in the expression of both Kv4.2 and KChIP2 [10], we further assessed regional variations of $I_{to,f}$ in the Kv4.2-/- hearts. In order to evaluate transmural heterogeneity of $I_{to,f}$, K^+ currents were recorded from epicardial (EPI) cardiomyocytes from the left ventricular free wall. The analysis revealed, that the density of I_{to} was larger in the EPI cardiomyocytes than ENDO cardiomyocytes in both WT and Kv4.2-/- hearts (Fig 5A and Table 1). More importantly, this transmural I_{to} pattern was entirely due to differences in the fast components of $I_{to,f}$ (Table 2). After separating $I_{to,f}$ and $I_{to,s}$ as shown above in Fig 5B, $I_{to,f}$ density in EPI was ~4-fold bigger than in ENDO in WT, while it only ~1.2-fold bigger in EPI than ENDO in Kv4.2-/- (Fig 5C). Thus, while Kv4.2 appears to be a major determinant of the $I_{to,f}$ transmural gradient in mouse myocardium, a residual transmural $I_{to,f}$ gradient remains in Kv4.2-/- and is associated with a corresponding the gradient ($P = 0.0418$) of KChIP2, but not ($P = 0.7214$) Kv4.3, mRNA expression. Interestingly, the transmural Kv4.3 mRNA gradient in the Kv4.2-/- hearts did not differ ($P = 0.8633$) from that in the WT hearts (Fig 6).

Discussion

Our results establish that, when long depolarization pulses (25 sec), $I_{to,f}$ can be readily identified. This conclusion clearly contrasts with a previous study [11] concluding that $I_{to,f}$ is absent in Kv4.2-/- hearts. We believe the lack of agreement can be readily explained by differences in

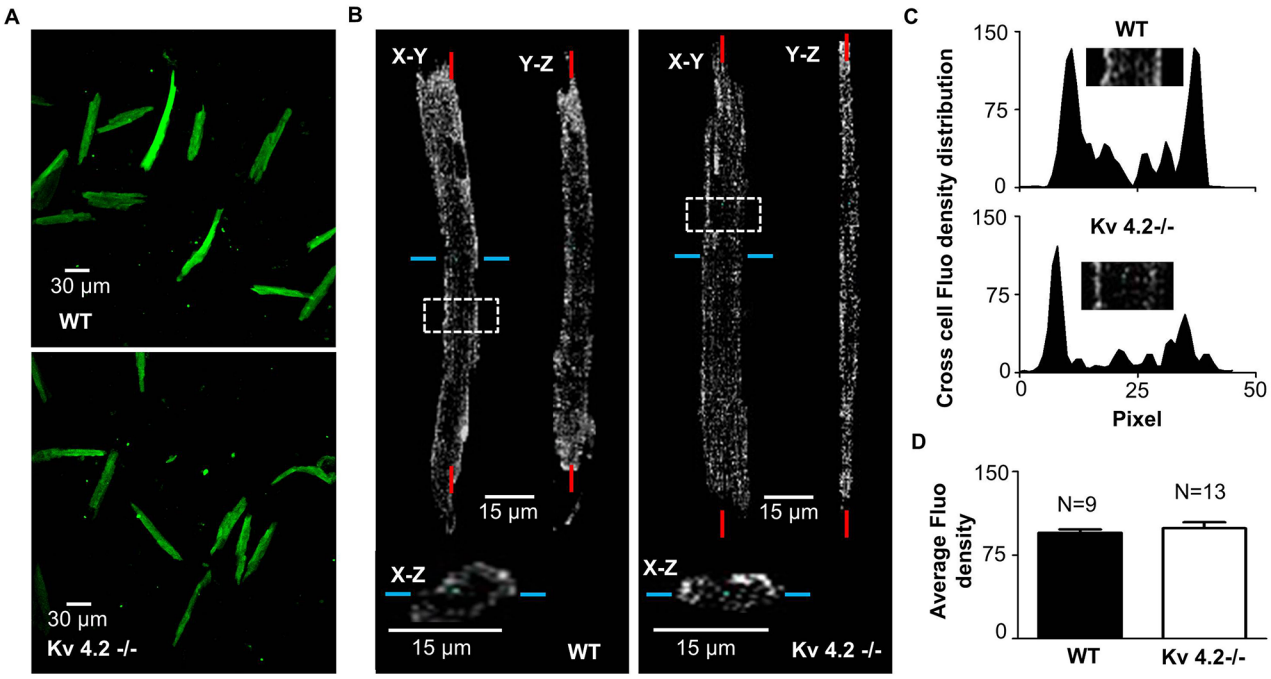

Fig 4. Membrane expression of Kv4.3 subunit in isolated WT and Kv4.2-/- cardiomyocyte. (A) Adult WT (top panel) and Kv4.2-/- (bottom panel) mouse ventricular cardiac myocytes labeled with anti-Kv4.3 antibody show positive fluorescent staining (originating from the 2nd antibody) at 10X magnification. (B) This panel shows the 3D reconstruction of a series of Z-stack fluorescent images of a typical cardiomyocyte taken using a confocal microscope. In the upper part of the figure the fluorescence pattern is shown for cardiomyocytes in two longitudinal orientations (X-Y and Y-Z planes). A cross-section was take through the cardiomyocytes at the position indicated by the blue line and is shown in the bottom (the X-Z plane). The results clearly demonstrate that the fluorescent signals originate primarily from the regions at the periphery for both WT (left panel) and Kv4.2-/- (right panel) cardiomyocytes. (C) This shows the fluorescent density distribution across the WT and a Kv4.2-/- cardiomyocyte shown in Panel B in the regions identified by the white boxes. (D) This quantifies the average integrated fluorescence density for cardiomocytes from WT (n = 9 cardiomyocytes from 4 hearts) and Kv4.2-/- (n = 13 cardiomyocytes from 6 heart) hearts. Average fluorescent density was calculated by summing the total fluorescent signal intensity normalized for the total number of pixels for each cardiomyocyte. Note this quantifies and the Kv4.3-subunit expression level in each cardiomyocyte.

doi:10.1371/journal.pone.0133274.g004

the voltage protocols and methods of quantifying the time dependent K^+ current traces. Specifically, in a previous study [13] we showed that, when K^+ current traces are lasting ~25 s, K^+ current traces are best fit with tri-exponential functions. This conclusion can be readily illustrated by showing that the distribution of the τ_{inact} values obtained from tri-exponential fits are much "tighter" (i.e. smaller variance) than when either bi-exponential or quadri-exponential fits to the traces were used [13]. Our results further showed that the estimates of the magnitude and time constants of the different current components become increasingly inaccurate as the length of the traces (used for the fits) are shortened. These observations are consistent with our analysis showing that tri-exponential functions gave the best statistical fits to the K^+ current traces [31]. We confirmed these findings in the Kv4.2-/- cardiomyocytes (data not shown) and found further that only the component with fastest time constant (i.e. τ_{inact} for I_{to}) differed with WT cardiomyocytes. One potential complication when using long depolarization pulses is K^+ ion depletion which could impact on the measured kinetics of K^+ current decay during the depolarizing pulses. However, the resting membrane potentials did not differ immediately before and after the long depolarizing pulses (i.e. before -72.38 ± 0.29 mV, n = 200 vs. after -72.38 ± 0.29 mV, n = 200; S1 Table). These observations are not unexpected since the amount of K^+ that is able to diffuse from the pipette (1.2~ 2 MΩ, 1~3 μm tip) into the cell is predicted, from the application of Fick's Law of Diffusion [32, 33], to be at least 10-fold greater than the amount of K^+ that leaves the cardiomyocytes through K^+ channels (i.e. $2.92 \pm 0.09 \times 10^{-7}$

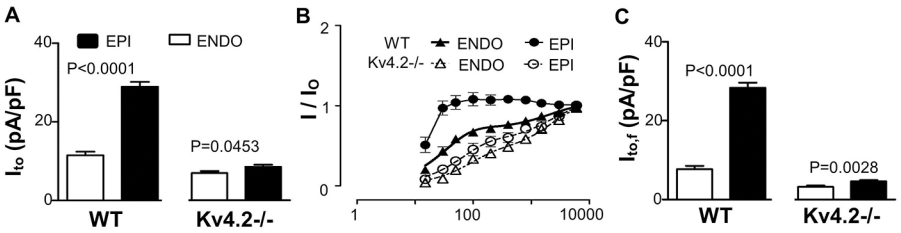

Fig 5. Heterogeneity of I_{to} and $I_{to,f}$ in left ventricular free wall cardiomyocytes in WT and Kv4.2-/-. (A) This shows the average I_{to} density ($I_{to} = I_{to,f} + I_{to,s}$) estimated in EPI and ENDO cardiomyocytes isolated from WT and Kv4.2-/- hearts (n = 12 for all groups) using the tri-exponential fitting protocol (described in Fig 1). As we can see, I_{to} density in Kv4.2-/- was reduced compared to WT for both ENDO and EPI cardiomyocytes. What is striking here is that the transmural gradients of I_{to} (EPI/ENDO) exist in left ventricular free walls for both WT and Kv4.2-/- but this gradient is markedly reduced in the Kv4.2-/- compared to WT. (B) Again I_{to} recovery from inactivation curve (n = 12 in each group) was used to separate $I_{to,f}$ and $I_{to,s}$ in I_{to} using the method described in Fig 2. (C) This panel quantifies the $I_{to,f}$ measured in ENDO and EPI cardiomyocytes from WT and Kv4.2-/- hearts (n = 6 for all groups).

doi:10.1371/journal.pone.0133274.g005

Coulombs) during the depolarizing pulses under our experimental conditions. We are confident that the long depolarization pulses did not significantly distort the various K^+ currents or the conclusions derived from our analysis.

Although, as expected, the estimated density of $I_{to,f}$ was reduced in the Kv4.2-/- cardiomyocytes compared to WT, there were also notable difference in both the kinetics of inactivation (τ_{inact}) and recovery from inactivation (τ_{rec}) of $I_{to,f}$ between cardiomyocytes from Kv4.2-/- (τ_{inact} = ~105ms and τ_{tec} = ~87ms) versus for WT (τ_{inact} = ~58ms and τ_{rec} = ~34ms) hearts. The deceleration in the rates of inactivation and recovery from inactivation observed in Kv4.2-/- cardiomyocytes are consistent with slower intrinsic inactivation properties of Kv4.3-based currents compared to Kv4.2-based currents observed in heterologous expression systems [28]. Taken together, these results support the conclusion that $I_{to,f}$ in mouse cardiomyocytes can be formed by Kv4.3 alone, and does not require co-assembly of Kv4.2 and Kv4.3 [11]. This conclusion is further supported by our toxin studies showing that the highly selective blocker of Kv4 currents, HpTx-2, was reduced K^+ currents in Kv4.2-/- cardiomyocyte during the first 400 ms after depolarization only, which is the period during which $I_{to,f}$ is expected to be active (i.e. not inactivated). Moreover, the densities of the HpTx-2-sensitive current were

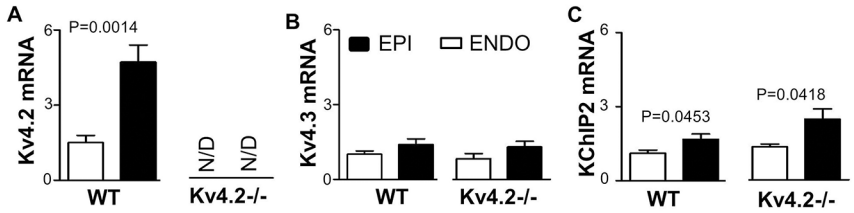

Fig 6. Kv4.2, Kv4.3 and KChIP2 mRNA expression level in ENDO and EPI tissue sample from left ventricular free wall of WT and Kv4.2-/- hearts. Relative gene expression of voltage-gated K^+ channels in ENDO and EPI tissues of WT (n = 6) and Kv4.2-/- (n = 6) hearts were measured by qtPCR and analyzed using the ΔΔCt method with normalization to GAPDH, which did not change between samples. The qtPCR protocols involved 35 cycles for all reactions. All the primers were tested with by generating standard curves to measure probe efficiency and both meting curves and electrophoresis were utilized to confirm single PCR products. (A) This panel shows the estimated Kv4.2 mRNA expression levels detected in WT hearts. No specific Kv4.2 PCR product was detected in Kv4.2-/- hearts after 35 cycles (i.e. not detected, ND). Note the large EPI to ENDO gradients in the WT hearts, as expected. (B) Kv4.3 mRNA expression in both WT and Kv4.2-/- hearts showing no measureable gradient, although trends existing with more in the EPI than ENDO. (C) KChIP2 mRNA showing transmural heterogeneity (EPI>ENDO) in both the WT and Kv4.2-/- hearts.

doi:10.1371/journal.pone.0133274.g006

indistinguishable from the $I_{to,f}$ estimated from the analysis of our curve fits to the voltage-gated K^+ currents. In addition, the HpTx-2-sensitive currents in Kv4.2-/- cardiomyocytes had decay properties that were also slower than in WT cardiomyocytes, as expected if $I_{to,f}$ in the Kv4.2-/- cardiomyocytes is comprised of Kv4.3-based channels [28]. HpTx-2 also eliminated the fast recovering component of I_{to} in our recover from inactivation measurements (i.e. $I_{to,f}$) in both WT and Kv4.2-/-, which uncovered mono-exponential slow recovering component (i.e. $I_{to,s}$) in both groups with identical magnitudes and kinetics. Our conclusion that $I_{to,f}$ does not require Kv4.2/3 co-assembly in mouse myocardium is supported by a recent study showing that $I_{to,f}$ is detectable in cardiomyocytes from mice lacking Kv4.3, which showed accelerated rates of inactivation compared to wild-type [12]. This conclusion is also consistent with the observation in Western Blots that the Kv4.3 protein (and mRNA) are present in Kv4.2-/- hearts at levels equivalent to that in WT hearts [11]. We confirmed that no significant differences in either Kv4.3 mRNA expression and or Kv4.3 protein in the membranes as measured immunohistochemically between Kv4.2-/- and WT cardiomyocytes.

Another novel finding of our studies is the identification of a transmural gradient in the Kv4.2-/- hearts. Previous studies have established that the gradients of $I_{to,f}$ underlie regional differences in the amplitude and kinetics of contraction in rodent [34, 35] and dog [36] hearts, which are predicted to synchronize contraction across the ventricular wall [1]. Regardless, the $I_{to,f}$ gradient in the Kv4.2-/- hearts was associated with a gradient in KChIP2, as we can see its expression seems increase a little in Kv4.2-/- in Fig 6, but not Kv4.3 expression. These observations suggest that the KChIP2 gradient can contribute to the transmural $I_{to,f}$ gradient in mouse hearts, as appears to be the case in dogs [9] and humans [37] which both do not express Kv4.2 [24, 29]. However, a recent study has linked Kv4.2 mutations to cardiac arrhythmias [38]. Consistent with previous mouse studies [10] and unlike dog hearts [37], we did not see a transmural gradient of Kv4.3 expression in the mouse heart, although a trend ($P = 0.1984$) did exist for a gradient. Taken together, the observation that the transmural $I_{to,f}$ gradient exists, albeit with a reduced magnitude, in Kv4.2-/- hearts compared to WT hearts, supports the conclusion that both Kv4.2 and KChIP2 contribute to the $I_{to,f}$ gradient in the mouse heart.

Since the Kv4.2-/- heart expresses Kv4.3-dependent $I_{to,f}$ like in humans cardiomyocytes, these mice might be useful for studying the regulation and consequences of $I_{to,f}$ in humans who do not appear to express Kv4.2, although Kv4.2 mutation was associated with a single patient with J-wave syndrome [38]. This suggestion is bolstered by the observation that $I_{to,f}$ levels and $I_{to,f}$ channel gene expression change similarly between humans and mice in both heart disease and during heart development [3, 39–41]. Moreover, despite the fact that the action potentials durations may differ by ~10-fold between these species, the effects of changes in $I_{to,f}$ are primarily limited to the early notch of the action potential in human cardiomyocyte which are predicted to be associated with alterations in $I_{Ca,L}$ current profiles and thereby excitation-contraction coupling as seen in mice and other species [1, 42–46]. Future studies will be required to assess whether the Kv4.2-/- mice are a useful model for further understanding $I_{to,f}$ in humans, and how the change of $I_{to,f}$ affect the expression and function of Kv1.4, Kv2.1 and Kv1.5-encoded channels and currents.

Supporting Information

S1 Table. Effect of 25 s stimulation pulse on resting potential in cardiomyocytes. Resting potential in Kv4.2-/- and WT ventricular myocyte were measured with whole-cell patch-clamp technique before and immediately after 25s stimulation pulse at +60 mV. The resting potential did not changed immediately after stimulation pulse which suggests no significant intracellular

K^+ concentration changed by the stimulation pulse.
(XLSX)

Acknowledgments

The authors thank Roman Pekhletski, Anna Rosen, Adam Korogyi and Dongling Zhao for technical support and discussion. Kv4.2-/- mice were generously provided by Dr. Jeanne Nerbonne at Washington University Medical School.

Author Contributions

Conceived and designed the experiments: JL KHK PHB. Performed the experiments: JL KHK. Analyzed the data: JL KHK PHB. Contributed reagents/materials/analysis tools: MJM SPH. Wrote the paper: JL KHK CCH PHB.

References

1. Sah R, Ramirez RJ, Oudit GY, Gidrewicz D, Trivieri MG, Zobel C, et al. Regulation of cardiac excitation-contraction coupling by action potential repolarization: role of the transient outward potassium current (I(to)). The Journal of physiology. 2003; 546(Pt 1):5–18. Epub 2003/01/02. PMID: 12509475; PubMed Central PMCID: PMC2342473.
2. Kassiri Z, Zobel C, Nguyen TT, Molkentin JD, Backx PH. Reduction of I(to) causes hypertrophy in neonatal rat ventricular myocytes. Circulation research. 2002; 90(5):578–85. Epub 2002/03/23. PMID: 11909822.
3. Wickenden AD, Kaprielian R, Parker TG, Jones OT, Backx PH. Effects of development and thyroid hormone on K+ currents and K+ channel gene expression in rat ventricle. The Journal of physiology. 1997; 504 (Pt 2):271–86. Epub 1997/11/20. PMID: 9365903; PubMed Central PMCID: PMC1159909.
4. Rosati B, Pan Z, Lypen S, Wang HS, Cohen I, Dixon JE, et al. Regulation of KChIP2 potassium channel beta subunit gene expression underlies the gradient of transient outward current in canine and human ventricle. The Journal of physiology. 2001; 533(Pt 1):119–25. Epub 2001/05/15. PMID: 11351020; PubMed Central PMCID: PMC2278594.
5. Guo W, Li H, Aimond F, Johns DC, Rhodes KJ, Trimmer JS, et al. Role of heteromultimers in the generation of myocardial transient outward K+ currents. Circulation research. 2002; 90(5):586–93. Epub 2002/03/23. PMID: 11909823.
6. Kaprielian R, Sah R, Nguyen T, Wickenden AD, Backx PH. Myocardial infarction in rat eliminates regional heterogeneity of AP profiles, I(to) K(+) currents, and [Ca(2+)](i) transients. American journal of physiology Heart and circulatory physiology. 2002; 283(3):H1157–68. Epub 2002/08/16. doi: 10.1152/ajpheart.00518.2001 PMID: 12181147.
7. Niwa N, Nerbonne JM. Molecular determinants of cardiac transient outward potassium current (I(to)) expression and regulation. Journal of molecular and cellular cardiology. 2010; 48(1):12–25. Epub 2009/07/22. doi: 10.1016/j.yjmcc.2009.07.013 PMID: 19619557; PubMed Central PMCID: PMC2813406.
8. Bertaso F, Sharpe CC, Hendry BM, James AF. Expression of voltage-gated K+ channels in human atrium. Basic research in cardiology. 2002; 97(6):424–33. Epub 2002/10/24. doi: 10.1007/s00395-002-0377-4 PMID: 12395204.
9. Rosati B, Grau F, Rodriguez S, Li H, Nerbonne JM, McKinnon D. Concordant expression of KChIP2 mRNA, protein and transient outward current throughout the canine ventricle. The Journal of physiology. 2003; 548(Pt 3):815–22. Epub 2003/02/25. doi: 10.1113/jphysiol.2002.033704 PMID: 12598586; PubMed Central PMCID: PMC2342878.
10. Teutsch C, Kondo RP, Dederko DA, Chrast J, Chien KR, Giles WR. Spatial distributions of Kv4 channels and KChip2 isoforms in the murine heart based on laser capture microdissection. Cardiovascular research. 2007; 73(4):739–49. Epub 2007/02/10. doi: 10.1016/j.cardiores.2006.11.034 PMID: 17289005.
11. Guo W, Jung WE, Marionneau C, Aimond F, Xu H, Yamada KA, et al. Targeted deletion of Kv4.2 eliminates I(to,f) and results in electrical and molecular remodeling, with no evidence of ventricular hypertrophy or myocardial dysfunction. Circulation research. 2005; 97(12):1342–50. Epub 2005/11/19. doi: 10.1161/01.RES.0000196559.63223.aa PMID: 16293790.

12. Niwa N, Wang W, Sha Q, Marionneau C, Nerbonne JM. Kv4.3 is not required for the generation of functional Ito,f channels in adult mouse ventricles. Journal of molecular and cellular cardiology. 2008; 44 (1):95–104. Epub 2007/11/30. doi: 10.1016/j.yjmcc.2007.10.007 PMID: 18045613; PubMed Central PMCID: PMC2245858.

13. Liu J, Kim KH, London B, Morales MJ, Backx PH. Dissection of the voltage-activated potassium outward currents in adult mouse ventricular myocytes: I(to,f), I(to,s), I(K,slow1), I(K,slow2), and I(ss). Basic research in cardiology. 2011; 106(2):189–204. Epub 2011/01/22. doi: 10.1007/s00395-010-0134-z PMID: 21253754.

14. Zhou J, Kodirov S, Murata M, Buckett PD, Nerbonne JM, Koren G. Regional upregulation of Kv2.1-encoded current, IK,slow2, in Kv1DN mice is abolished by crossbreeding with Kv2DN mice. American journal of physiology Heart and circulatory physiology. 2003; 284(2):H491–500. Epub 2003/01/17. doi: 10.1152/ajpheart.00576.2002 PMID: 12529256.

15. Chen X, Yuan LL, Zhao C, Birnbaum SG, Frick A, Jung WE, et al. Deletion of Kv4.2 gene eliminates dendritic A-type K+ current and enhances induction of long-term potentiation in hippocampal CA1 pyramidal neurons. The Journal of neuroscience: the official journal of the Society for Neuroscience. 2006; 26(47):12143–51. Epub 2006/11/24. doi: 10.1523/JNEUROSCI.2667-06.2006 PMID: 17122039.

16. Zhang M, Jiang M, Tseng GN. minK-related peptide 1 associates with Kv4.2 and modulates its gating function: potential role as beta subunit of cardiac transient outward channel? Circulation research. 2001; 88(10):1012–9. Epub 2001/05/26. PMID: 11375270.

17. Faivre JF, Calmels TP, Rouanet S, Javre JL, Cheval B, Bril A. Characterisation of Kv4.3 in HEK293 cells: comparison with the rat ventricular transient outward potassium current. Cardiovascular research. 1999; 41(1):188–99. Epub 1999/05/18. PMID: 10325966.

18. Kim KH, Oudit GY, Backx PH. Erythropoietin protects against doxorubicin-induced cardiomyopathy via a phosphatidylinositol 3-kinase-dependent pathway. J Pharmacol Exp Ther. 2008; 324(1):160–9. Epub 2007/10/12. doi: 10.1124/jpet.107.125773 PMID: 17928571.

19. Menegola M, Trimmer JS. Unanticipated region- and cell-specific downregulation of individual KChIP auxiliary subunit isotypes in Kv4.2 knock-out mouse brain. The Journal of neuroscience: the official journal of the Society for Neuroscience. 2006; 26(47):12137–42. Epub 2006/11/24. doi: 10.1523/JNEUROSCI.2783-06.2006 PMID: 17122038.

20. Zhang SS, Kim KH, Rosen A, Smyth JW, Sakuma R, Delgado-Olguin P, et al. Iroquois homeobox gene 3 establishes fast conduction in the cardiac His-Purkinje network. Proceedings of the National Academy of Sciences of the United States of America. 2011; 108(33):13576–81. Epub 2011/08/10. doi: 10.1073/pnas.1106911108 PMID: 21825130; PubMed Central PMCID: PMC3158173.

21. Patel SP, Parai R, Campbell DL. Regulation of Kv4.3 voltage-dependent gating kinetics by KChIP2 isoforms. The Journal of physiology. 2004; 557(Pt 1):19–41. Epub 2004/01/16. doi: 10.1113/jphysiol.2003.058172 PMID: 14724186; PubMed Central PMCID: PMC1665034.

22. Deschenes I, DiSilvestre D, Juang GJ, Wu RC, An WF, Tomaselli GF. Regulation of Kv4.3 current by KChIP2 splice variants: a component of native cardiac I(to)? Circulation. 2002; 106(4):423–9. Epub 2002/07/24. PMID: 12135940.

23. Dilks D, Ling HP, Cockett M, Sokol P, Numann R. Cloning and expression of the human kv4.3 potassium channel. Journal of neurophysiology. 1999; 81(4):1974–7. Epub 1999/04/14. PMID: 10200233.

24. Zhu XR, Wulf A, Schwarz M, Isbrandt D, Pongs O. Characterization of human Kv4.2 mediating a rapidly-inactivating transient voltage-sensitive K+ current. Receptors & channels. 1999; 6(5):387–400. Epub 1999/11/07. PMID: 10551270.

25. Petersen KR, Nerbonne JM. Expression environment determines K+ current properties: Kv1 and Kv4 alpha-subunit-induced K+ currents in mammalian cell lines and cardiac myocytes. Pflugers Archiv: European journal of physiology. 1999; 437(3):381–92. Epub 1999/01/23. PMID: 9914394.

26. Matsubara H, Suzuki J, Inada M. Shaker-related potassium channel, Kv1.4, mRNA regulation in cultured rat heart myocytes and differential expression of Kv1.4 and Kv1.5 genes in myocardial development and hypertrophy. The Journal of clinical investigation. 1993; 92(4):1659–66. Epub 1993/10/01. doi: 10.1172/JCI116751 PMID: 7691883; PubMed Central PMCID: PMC288324.

27. Fedida D, Bouchard R, Chen FS. Slow gating charge immobilization in the human potassium channel Kv1.5 and its prevention by 4-aminopyridine. The Journal of physiology. 1996; 494 (Pt 2):377–87. Epub 1996/07/15. PMID: 8841998; PubMed Central PMCID: PMC1160641.

28. Guo W, Malin SA, Johns DC, Jeromin A, Nerbonne JM. Modulation of Kv4-encoded K(+) currents in the mammalian myocardium by neuronal calcium sensor-1. The Journal of biological chemistry. 2002; 277 (29):26436–43. Epub 2002/05/08. doi: 10.1074/jbc.M201431200 PMID: 11994284.

29. Dixon JE, Shi W, Wang HS, McDonald C, Yu H, Wymore RS, et al. Role of the Kv4.3 K+ channel in ventricular muscle. A molecular correlate for the transient outward current. Circulation research. 1996; 79 (4):659–68. Epub 1996/10/01. PMID: 8831489.

30. El-Haou S, Balse E, Neyroud N, Dilanian G, Gavillet B, Abriel H, et al. Kv4 potassium channels form a tripartite complex with the anchoring protein SAP97 and CaMKII in cardiac myocytes. Circulation research. 2009; 104(6):758–69. Epub 2009/02/14. doi: 10.1161/CIRCRESAHA.108.191007 PMID: 19213956.

31. Glover DM JW, Doney SC. Modeling methods for marine science. 2005; Cambridge University Press.

32. Fick A. Philosophical Magazine. 1855; 10.

33. Crank J. THE MATHEMATICS of DIFFUSION second edition, Clarendon press. 1975.

34. Sah R, Ramirez RJ, Kaprielian R, Backx PH. Alterations in action potential profile enhance excitation-contraction coupling in rat cardiac myocytes. The Journal of physiology. 2001; 533(Pt 1):201–14. Epub 2001/05/15. PMID: 11351028; PubMed Central PMCID: PMC2278610.

35. Fiset C, Giles WR. Transmural gradients of repolarization and excitation-contraction coupling in mouse ventricle. Circulation research. 2006; 98(10):1237–9. Epub 2006/05/27. doi: 10.1161/01.RES.0000225859.82676.ba PMID: 16728668.

36. Cordeiro JM, Greene L, Heilmann C, Antzelevitch D, Antzelevitch C. Transmural heterogeneity of calcium activity and mechanical function in the canine left ventricle. American journal of physiology Heart and circulatory physiology. 2004; 286(4):H1471–9. Epub 2003/12/13. doi: 10.1152/ajpheart.00748.2003 PMID: 14670817.

37. Zicha S, Xiao L, Stafford S, Cha TJ, Han W, Varro A, et al. Transmural expression of transient outward potassium current subunits in normal and failing canine and human hearts. The Journal of physiology. 2004; 561(Pt 3):735–48. Epub 2004/10/23. doi: 10.1113/jphysiol.2004.075861 PMID: 15498806; PubMed Central PMCID: PMC1665387.

38. Perrin MJ, Adler A, Green S, Al-Zoughool F, Doroshenko P, Orr N, et al. Evaluation of Genes Encoding for the Transient Outward Current (Ito) Identifies the KCND2 Gene as a Cause of J Wave Syndrome Associated with Sudden Cardiac Death. Circulation Cardiovascular genetics. 2014. Epub 2014/09/13. doi: 10.1161/CIRCGENETICS.114.000623 PMID: 25214526.

39. Nabauer M, Beuckelmann DJ, Erdmann E. Characteristics of transient outward current in human ventricular myocytes from patients with terminal heart failure. Circulation research. 1993; 73(2):386–94. Epub 1993/08/01. PMID: 8330381.

40. Holzem KM, Efimov IR. Arrhythmogenic remodelling of activation and repolarization in the failing human heart. Europace: European pacing, arrhythmias, and cardiac electrophysiology: journal of the working groups on cardiac pacing, arrhythmias, and cardiac cellular electrophysiology of the European Society of Cardiology. 2012; 14 Suppl 5:v50–v7. Epub 2012/11/01. doi: 10.1093/europace/eus275 PMID: 23104915; PubMed Central PMCID: PMC3697802.

41. Kaab S, Dixon J, Duc J, Ashen D, Nabauer M, Beuckelmann DJ, et al. Molecular basis of transient outward potassium current downregulation in human heart failure: a decrease in Kv4.3 mRNA correlates with a reduction in current density. Circulation. 1998; 98(14):1383–93. Epub 1998/10/07. PMID: 9760292.

42. Yan GX, Antzelevitch C. Cellular basis for the electrocardiographic J wave. Circulation. 1996; 93(2):372–9. Epub 1996/01/15. PMID: 8548912.

43. Calloe K, Cordeiro JM, Di Diego JM, Hansen RS, Grunnet M, Olesen SP, et al. A transient outward potassium current activator recapitulates the electrocardiographic manifestations of Brugada syndrome. Cardiovascular research. 2009; 81(4):686–94. Epub 2008/12/17. doi: 10.1093/cvr/cvn339 PMID: 19073629; PubMed Central PMCID: PMC2642600.

44. Grubb S, Calloe K, Thomsen MB. Impact of KChIP2 on Cardiac Electrophysiology and the Progression of Heart Failure. Frontiers in physiology. 2012; 3:118. Epub 2012/05/16. doi: 10.3389/fphys.2012.00118 PMID: 22586403; PubMed Central PMCID: PMC3343377.

45. Patberg KW, Plotnikov AN, Quamina A, Gainullin RZ, Rybin A, Danilo P, et al. Cardiac memory is associated with decreased levels of the transcriptional factor CREB modulated by angiotensin II and calcium. Circulation research. 2003; 93(5):472–8. doi: 10.1161/01.Res.0000088785.24381.2f PMID: ISI:000185135000014.

46. del Balzo U, Rosen MR. T wave changes persisting after ventricular pacing in canine heart are altered by 4-aminopyridine but not by lidocaine. Implications with respect to phenomenon of cardiac 'memory'. Circulation. 1992; 85(4):1464–72. Epub 1992/04/01. PMID: 1555287.